European Commission
FP7, Grant Agreement 211743

Review of displacement-noise-reduction techniques

ET-024-09

Sergey Tarabrin

Issue: 1

Date: October 12, 2009

Max-Planck-Institut für Gravitationsphysik
Callinstrasse 38, 30167 Hannover, Germany

Contents

1 Introduction

It is well-known that the sensitivity of the first-generation ground-based laser interferometric GW detectors is limited by the great amount of different types of noise. The most significant limiting factors at low frequencies (below $\sim$ 50 Hz) are gravity-gradient noise (variations in the local gravitational field), seismic noise (external mechanical vibrations transmitted to the test masses through their suspensions) and thermal noise in the mirrors suspensions. At middle frequencies ($\sim 50 \div 500$ Hz) thermal noise in the bulks and coatings of the mirrors dominate. At higher frequencies (above $\sim$ 500 Hz) photon shot noise limits the sensitivity. Therefore, all the noises up to $\sim$ 500 Hz can be referred to the class of displacement noise of the test masses.

In the second-generation detectors, being under preparation, all these noises still remain but their values are shifted downwards. This leads to the sensitivity limitation by the standard quantum limit (SQL). The cause of SQL is the fluctuating force of radiation pressure in the laser beam (back-action noise) pushing the interferometer mirrors in a random manner. Therefore, standard quantum limitation would disappear if one could remove displacement noise.

Each method of suppression or elimination of displacement noises proposed up-to-date is only suited for control of only one kind of noise. For instance, active seismic isolation will suppress seismic noise but is helpless against thermal noise or quantum radiation pressure. From the other hand, quantum-non-demolition (QND) schemes of measurements are able to cancel back-action noise but are certainly not suited for dealing with seismic or thermal noise. In this review we will discuss the method of displacement noise cancelation which aims at simultaneous elimination of the information about all external fluctuating forces but leaves a certain amount of information about the gravitational waves. This method is usually referred to as displacement-noise-free interferometry (DFI) in literature. DFI implies that, in principle, test masses no longer need to be isolated from the environment or cooled to low temperatures. In addition, elimination of radiation pressure implies that DFIs are no longer limited by the SQL. This can be thought of an alternative method to overcome SQL which, contrary to QND, is not strongly vulnerable to optical losses. If all displacement noises are eliminated, the sensitivity of DFIs is ultimately limited by the shot noise.

DFI was first proposed by S. Kawamura and Y. Chen in [1]. In that paper a toy model consisting of three test masses exchanging the electromagnetic signals with each other was considered. It was shown that it is possible, in principle, to combine timing signals in such a way that the combination does not include displacement noise but preserves the GW signal. The reason for this is that the optical GW detector responds differently to the motions of the test masses and the GW. The "payment" for displacement noise cancelation is the reduction of GW response at low frequencies.

In the following paper [2] the authors included timing noises in the consideration and analyzed a conversion of their toy model into interferometric schemes. It was argued that in order to perform complete displacement noise cancelation, laser noise must also be canceled since it is indistinguishable from displacement noise. The theorem was proven stating that DFI is impossible in a one-dimensional system, i.e. whenever laser **and** displacement noises are canceled, the GW signal vanishes. For two- and three-dimensional schemes DFI is possible with at least 5 and 6 test masses, respectively.

In the next paper [3] two practical interferometric designs were considered, namely two- and three- dimensional schemes for ground- and space-based detectors, respectively. For these schemes the authors found that the GW transfer function is $(L/\lambda_{\rm GW})^n$ ($n = 2$ for 3D, $n = 3$ for 2D and L is the linear scale of the GW detector) times weaker than the transfer function of conventional Michelson interferometer at low frequencies (when $L \ll \lambda_{\rm GW}$). Therefore, major advantages of DFIs are leveled by significant reduction of GW susceptibility in astrophysically most interesting frequency region.

It was argued [4] that in order to increase the GW response, time-delaying devices should be inserted into the arms of displacement-noise-free interferometers. However, it was found that the improvement in the GW response can only be achieved if the noise in the time-delay devices is not canceled. Therefore, the net sensitivity becomes limited by this noise and DFI loses its advantages.

Another direction in the development of displacement noise reduction was taken in paper [5]. As a first step

a toy model of a single Fabry-Perot cavity was considered. It was proposed to pump the cavity from both sides and monitor reflected and transmitted waves. It was found that due to the effect of prompt reflection it is possible to obtain the GW transfer function proportional to $(L/\lambda_{\rm GW})^0$ and cancel displacement noise of the cavity mirrors. However, sensitivity becomes limited by the displacement noise of lasers, photodetectors and all the auxiliary optics. In addition, a single-cavity scheme does not allow laser noise cancelation.

In order to get rid of residual displacement noise a double-cavity scheme was proposed in [6]. This scheme is similar to the initial toy model in paper [1]. The difference is that highly reflective mirrors are mounted on each test mass, thus, forming two symmetrically positioned cavities. It was shown that the proper linear combination of the responses allows complete displacement noise cancelation but at the cost of reduction of the GW susceptibility. It was found that at low frequencies the GW transfer function is proportional to $(L/\lambda_{\rm GW})(f_{\rm GW}\tau^*_{\rm FP})$, where $\tau^*_{\rm FP}$ is the cavity relaxation time. Therefore, cavity-based DFI has the GW susceptibility increased by the resonant gain of the cavities, as compared to the schemes proposed in paper [3]. Unfortunately, the assumption of the mirrors being rigidly mounted on some platforms limits practical value of such a scheme. Besides, laser noise still remains uncanceled.

In paper [7] a resonant speed meter interferometer was proposed allowing narrow-band displacement-noise-free GW detection. The mechanism of displacement noise cancelation is the same as in Sagnac-type interferometers. In paper [8] this model was converted into the wide-band detector by introducing an additional pump. The low-frequency response to GWs of such a detector is proportional to $f_{\rm GW}\tau^*_{\rm FP}$, where $\tau^*_{\rm FP}$ is the relaxation time of ring cavity. Evidently this quantity can be made of the order of unity. Another advantage of the wide-band speed meter DFI is the automatic cancelation of laser noise. However, the net sensitivity is limited by the displacement noise of the auxiliary beamsplitters and mirrors which are used to produce the pumping waves of the ring cavity.

In the most recent paper [9] symmetric feature of the double-cavity scheme has been combined with a laser noise cancelation technique. Namely, the proposed scheme consists of two symmetrically positioned Michelson/Fabry-Perot interferometers having a common central platform. The major disadvantage of this model is the need to place the beamsplitters and the input mirrors of the cavities on the common central platform. The GW transfer function is proportional to $(L/\lambda_{\rm GW})$. The only limiting noise source is the noise of local oscillators which are used for detection of the transmitted waves in the arms. Currently, this is the best one can achieve with the cavity-based DFI. However, there are certain indications that the severe model assumptions of the rigid platforms could be overcome in an interferometer with a multi-frequency pump. Several carrier frequencies increase the number of channels which can be used to eliminate more fluctuative degrees of freedom.

In the following section we will describe the basic physical mechanism underlying displacement-noise cancelation and briefly consider the DFI schemes proposed in literature with their advantages and disadvantages. It seems that currently none of the proposed schemes can be directly realized in practice. Further improvements and modifications are necessary, for instance, studying the possibilities which multi-frequency pump may give.

2 Displacement-noise-free interferometry

2.1 Basic mechanism

The basic idea of displacement-noise-free interferometry can be best explained from the viewpoint of a local observer. A natural observer in the GW experiment is the photodetector which produces an experimentally observable quantity. Let us assume for simplicity that this observer is freely falling in the GW field and is not subjected to non-GW fluctuative forces. In this case we can describe the interaction between the GW and the interferometer in the local Lorentz frame of that observer. General math and the case of a non-inertial observer can be found in Appendix A.

Assume that the interferometer is composed of several test masses. In the local Lorentz frame the interaction of the GW with a laser interferometer adds up to two effects. The first one is the motion of the test masses in the GW tidal force-field. In this aspect GWs are indistinguishable from any non-GW forces since both are sensed by the light wave only at the moments of reflection from the test masses. We will refer to this as the *localized* nature of the forces acting on the test masses. If the linear scale L of a GW detector is much smaller than the gravitational wavelength $\lambda_{\rm GW}$ (the so-called long-wave approximation) then the effect of the GW force-field is of the order of $h(L/\lambda_{\rm GW})^0$, where h is the absolute value of the GW amplitude. Relative motion of the test masses, separated by a distance L, in any force field cannot be sensed by one of them faster than L/c, thus resulting in the rise of terms of the order of $O[h(L/\lambda_{\rm GW})^1]$ describing time delays which take the light wave to travel between the masses. Second, the GW directly couples to the light wave effectively changing its coordinate velocity, thus manifesting itself as an effective refraction index. A light wave traveling in such a (boundless) medium acquires the information about the GW in its phase gradually, therefore it is a *distributed* effect having the $O[h(L/\lambda_{\rm GW})^2]$ order in long-wave approximation. Therefore, from the viewpoint of a local observer displacement-noise-free interferometry implies cancelation of localized effects (GW and non-GW forces) leaving a non-vanishing information about the distributed effect (the direct coupling of the GW to light).

Mind that usually laser noise dominates over other sources of noise in practice. Even if the lasers with highly suppressed technical noise (shot-noise-limited) are provided, any relative motions between the laser and other optical elements will recreate laser frequency noise via Doppler effect. Therefore, optical and displacement noise of a laser are indistinguishable from each other. This implies that DFI should also cancel laser noise.

In paper [2] the following theorem was proven. Imagine a system consisting of N test masses exchanging electromagnetic signals with each other and measuring time of reception by the proper clocks. This gives us $N(N-1)$ channels of timing signals. Each test mass is free to move in D spacial dimensions, where $D=1$ for a colinear configuration of the system, $D=2$ for coplanar and $D=3$ for generic configuration. Each of the N clocks also has intrinsic timing noise. Totally this gives us $ND+N$ channels of noise. In principle, it is possible to construct at least $N(N-1)-N(D+1)=N(N-D-2)$ timing combinations that are insusceptible to *all* displacement and timing noises if $N>D+2$. However, this does not guarantee that all these combinations will have non-vanishing response to GWs. It was proven that the 1D configurations have vanishing GW sensitivity and, thus, DFI is impossible in linear setups. 2D and 3D configurations allow DFI with at least 5 and 6 test masses, respectively.

2.2 Interferometers for complete displacement noise cancelation

As a demonstration of the proven theorem two examples of interferometers with complete displacement noise cancelation were considered in paper [3]. The 3D configuration (Octahedron) is depicted in Fig. 1. The interferometer is composed of four Mach-Zehnder interferometers A1, B1 (solid curves), A2 and B2 (dashed curves) with corresponding input ports $\mathrm{IN_{A1}}$, $\mathrm{IN_{B1}}$, $\mathrm{IN_{A2}}$ and $\mathrm{IN_{B2}}$. Corresponding output ports $\mathrm{OUT_{A1}}$, $\mathrm{OUT_{B1}}$, $\mathrm{OUT_{A2}}$ and $\mathrm{OUT_{B2}}$ are tuned to zero mean intensity. All arms are assumed to have equal length. Mirrors A and B are half-transparent, while mirrors $\mathrm{C_1}$, $\mathrm{C_2}$, $\mathrm{D_1}$ and $\mathrm{D_2}$ are absolutely reflective.

The response signals of four interferometers are recorded and then electronically post-processed. The difference in the responses of A1 and B1 cancels the displacement noise of mirrors $\mathrm{C_1}$ and $\mathrm{D_1}$ due to the equality of the

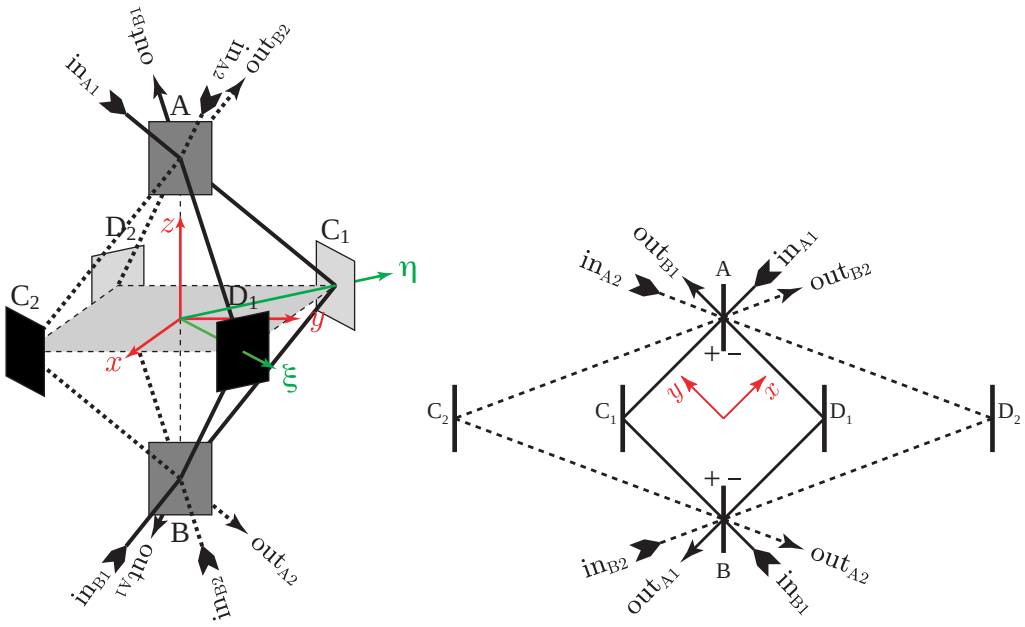

Figure 1: 3D and 2D displacement-noise-free interferometers performing displacement-noise-free GW detection.

arms. Similarly, the difference in the responses of A2 and B2 cancels the displacement noise of mirrors C_2 and D_2. Finally, the difference of these two combinations eliminates the motions of both beamsplitter A and B, since the interferometers A1 and A2 sense the motions of the beamsplitters in the same way as the interferometers B1 and B2.

Note that since the Octahedron is composed of Mach-Zehnder interferometers with detection in dark ports, laser noise is canceled automatically. The response to GWs corresponding to the described DFI combination turns out to be proportional to $h(L/\lambda_{\rm GW})^2$, where L is the length of interferometer arms. This is the direct consequence of the DFI mechanism: together with displacement noise we also cancel the GW-induced displacements which are of the $O[h(L/\lambda_{\rm GW})^0]$ order; only distributed effect described by $O[h(L/\lambda_{\rm GW})^2]$ remains.

The Octahedron configuration can be immediately "squeezed" into the 2D (see Fig. 1). Analysis shows that the DFI response to GWs of 2D scheme is proportional to $h(L/\lambda_{\rm GW})^3$.

It is useful to make some numerical estimates. As a reference for comparison we will use a single-pass Michelson interferometer (w/out arm cavities) and assume its GW susceptibility equal to unity. For $L = 10$ km and $f_{\rm GW} = 100$ Hz the susceptibilities of 3D and 2D DFI are $(L/\lambda_{\rm GW})^2 \approx 10^{-5}$ and $(L/\lambda_{\rm GW})^3 \approx 10^{-7}$ weaker than the one of Michelson interferometer with the same arm length.

The following factors which can limit the DFI sensitivity were mentioned in paper [3].

1. If the interferometer arms are not ideally equal but are kept with accuracy of δL then the displacement-noise reduction factor will be limited by $\delta L/L$ in amplitude.
2. If the beamsplitters are not ideally 50/50 then the limitation of reduction factor will be of the order of $|R_{\rm BS} - T_{\rm BS}|$, where $R_{\rm BS}$ and $T_{\rm BS}$ are beamplitters' power reflectivity and transmissivity.
3. Optical losses in the mirrors will limit noise reduction factor by ϵ in amplitude, where ϵ is the power loss coefficient.

In paper [4] it was proposed to utilize the artificial time-delay devices (for instance, medium with electromagnetically induced transparency) in order to increase the effective temporal size of the interferometer[1]. It is expected

[1]Fabry-Perot cavities and delay lines, for instance, increase the effective spacial size of an interferometer.

that this would lead to the increase of the low-frequency GW susceptibility. However, it was demonstrated that this can only be achieved if the noise in time-delay noises is not canceled. Therefore, the net sensitivity in almost the entire frequency band becomes limited with the time-delay noise.

3 Partial displacement noise cancelation with cavities

3.1 Limitations imposed by relativity principle

It is useful to look at the mechanism of DFI from another angle. Imagine again a system of test masses exchanging electromagnetic signals with each other. Any test mass can be chosen to be the local observer making local measurements inside the system. For instance, in the case of an interferometer the local observer is usually assigned to one of the interferometer's photodetectors. We will also assume that there exists a global inertial reference frame (which we will address as the laboratory frame) with corresponding (laboratory) observer. For instance, if the interferometer is placed underground then the laboratory frame can be associated with the cavern. The major difference between the laboratory frame and the proper frame of the local observer is that a laboratory observer is able to measure the common displacement and the common velocity of the system with respect to the laboratory, while a local observer is only able to measure the common acceleration of the system according to the relativity principle.

Let us choose one of the test masses as the reference mass (local observer) and some other j-th test mass as the probe. We denote the displacement of the probe test mass with respect to the laboratory frame as $\xi_j(t)$. Similar displacement of the reference test mass is $\xi_{\rm ref}(t)$. Clearly, the laboratory observer is able to measure $\xi_j(t)$ and $\xi_{\rm ref}(t)$ separately. However, the local observer is only able to measure the relative displacement of the j-th test mass with respect to its (observer's) frame. This displacement equals to $\delta x_j(t) = \xi_j(t) - \xi_{\rm ref}(t)$.

Mind that in the LL frame of the local observer a GW acts on the test masses like a tidal force in flat space-time. In the GW tidal field the probe mass moves with respect to the reference mass as $\delta x_j(t) = \frac{1}{2}x_0 h(t) + \xi_j(t) - \xi_{\rm ref}(t)$, where x_0 is the distance between the two masses in the state of rest and $h(t)$ is the GW function. The first term here, $\frac{1}{2}x_0 h(t)$, is the GW-induced displacement of the probe mass with respect to the reference one. Both $\xi_j(t)$ and $\xi_{\rm ref}(t)$ represent the displacement noise.

Now, suppose the system of the test masses represents an interferometric GW detector. Displacement-noise-free interferometry implies elimination of $\xi_{\rm ref}(t)$ and $\xi_j(t)$ for all j in the proper linear combination of the interferometer responses. However, the result of displacement noise elimination cannot be proportional to $x_0 h(t)$, since this would mean that we are somehow able to measure the absolute GW-displacement with respect to the global inertial frame using only the constituent parts of the system. This clearly contradicts the relativity principle. Below we call the response proportional to $x_0 h$ the zeroth order response, since it can be rewritten as $x_0 h (x_0/\lambda_{\rm GW})^0$. Therefore, if the zeroth order response is obtained in some combination of the responses then it will also contain several $\xi_{\rm ref}(t)$ representing the displacements of several reference test masses that have been used. This means that complete DFI is incompatible with the 0th order response due to the relativity principle. The same also holds true for the 1st order response, since absolute velocity measurements are also forbidden. The case of the 2nd and higher order responses $x_0 h (x_0/\lambda_{\rm GW})^n$ requires taking into account distributed redshift of the optical wave in the GW field.

The practical significance of the 0th and the 1st order incomplete DFIs can be achieved if residual displacement noises can be suppressed somehow by technical means, making them smaller than the GW signal.

3.2 Single-cavity scheme with the zeroth order response

The idea of displacement-noise-free GW detection is based on the fact that optical interferometers respond differently to the fluctuative motions of the test masses and the GWs. In principle, this difference can be of various nature. For instance, in conventional DFIs this difference owns to the distributed nature of the GWs compared to the localized nature of displacement noise. Therefore, if several response signals asymmetrically containing GW and displacement noise are provided, then it is possible, in principle, to separate the GW terms from *some* displacement noise terms. In certain cases it is possible to separate GW completely. This is only possible for the DFIs with the 2nd order GW response, for instance the Mach-Zehnder-type interferometer considered in Sec. 2.2. For the 0th and the 1st order responses only partial cancelation of displacement noise

is possible, as discussed above. Here we will discuss the scheme based on a single Fabry-Perot cavity with the 0th order response and the asymmetry between the responses based on the effect of prompt reflection.

Consider a system illustrated in Fig. 2a: a FP cavity assembled of two movable, partially transparent, mirrors a and b is pumped by a laser L_1 through mirror a. Detectors D_1 and D_2 measure the phases of reflected and

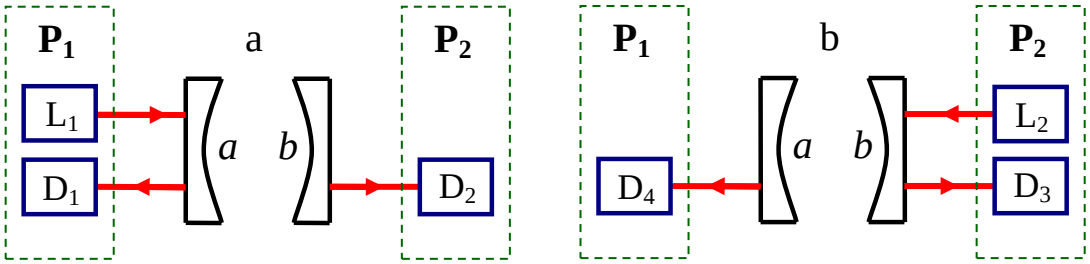

Figure 2: Cancelation of cavity noise.

transmitted waves correspondingly. For simplicity we assume that laser L_1 and detector D_1 are rigidly mounted on platform P_1 and detector D_2 is rigidly mounted on platform P_2. It is evident that the wave circulating inside the cavity measures the relative displacement of mirrors a and b plus GW displacement: $\xi_{\rm gw} + \xi_b - \xi_a$. The transmitted signal $a^{\rm t}_{\rm out}$ can be measured in such a way that it will be directly proportional to this quantity:

$$a^{\rm t}_{\rm out} = q_1(\xi_{\rm gw} + \xi_b - \xi_a). \tag{1a}$$

Here q_1 describes the resonant gain (amplification of the phase shift) of the cavity. The reflected signal $a^{\rm r}_{\rm out}$ is somewhat different: it also includes the component due to the prompt reflection of the pump wave from the input mirror. For instance, if the cavity is pumped through mirror a then this component is proportional to $\xi_a - \xi_{\rm P_1}$. The reflected signal is then

$$a^{\rm r}_{\rm out} = p(\xi_a - \xi_{\rm P_1}) + q_2(\xi_{\rm gw} + \xi_b - \xi_a). \tag{1b}$$

Here q_2 also describes the resonant gain (multiple reflections inside the cavity), while p is the quantity of the order of unity since it describes a single reflection from the input mirror. Equations (1a) and (1b) tell us that we are unable to measure absolute values of ξ_a and ξ_b, only relative measurements, e.g. with respect to platform P_1, are allowed.

Now consider the situation illustrated in Fig. 2b: the same cavity is pumped by laser L_2 through mirror b with the wave polarized normally to the wave emitted by laser L_1. Detectors D_3 and D_4 measure the phases of reflected and transmitted waves, resectively. Again we assume that laser L_2 and detector D_3 are rigidly mounted on platform P_2 and detector D_4 is rigidly mounted on platform P_1. The second pair of response signals can be derived in full similarity. Let us consider the simplest case of equal pumps (equal amplitudes and detunings). Then due to the symmetry of the system and plane GW wavefront the second pair of responses can be written as:

$$b^{\rm t}_{\rm out} = q_1(\xi_{\rm gw} + \xi_b - \xi_a), \tag{2a}$$
$$b^{\rm r}_{\rm out} = p(\xi_{\rm P_2} - \xi_b) + q_2(\xi_{\rm gw} + \xi_b - \xi_a). \tag{2b}$$

Here the displacements of the mirrors are measured with respect to platform P_2.

Now constructing the following linear combination of the responses

$$s = a^{\rm r}_{\rm out} + \frac{p - q_2}{q_1}\, a^{\rm t}_{\rm out} + b^{\rm r}_{\rm out} - \frac{q_2}{q_1}\, b^{\rm t}_{\rm out}, \tag{3}$$

we are able to cancel displacement noise of both mirrors:

$$s = p(\xi_{\rm gw} + \xi_{\rm P_2} - \xi_{\rm P_1}). \tag{4}$$

Note that the displacement noise of the platforms cannot be eliminated. This is the direct consequence of the relativity principle which states that no absolute coordinate or velocity measurements are allowed: one can measure the coordinates of the mirrors only with respect to the positions of reference test masses, platforms P_1 and P_2 in our case. Therefore, it is natural that their displacement noises impose the sensitivity limit.

According to formula (4), noise cancelation with the 0th order response is possible due to *the effect of prompt reflection* from the input mirror which is described by the p-multiplier. The obtained DFI response is similar to the response of a simple single-pass GW detector: an observer sends the light wave to the reflective mirror and receives it back measuring the phase shift. The noise-cancelation algorithm that we perform for a double-pumped FP cavity in some sense can be interpreted as removal of the cavity "by hands". Evidently, this results in the loss of the optical resonant gain: signal s in formula (4) includes neither q_1 nor q_2.

Two special cases when noise cancelation with the 0th order response is impossible can be immediately "predicted" from Eqs. (1a — 2b): (i) $p = 0$, meaning that the prompt reflection does not occur (this takes place for the resonant pump) and (ii) $\xi_a = \xi_{P_1}$ and simultaneously $\xi_b = \xi_{P_2}$, meaning that the mirrors are rigidly attached to the platforms.

In a more rigorous treatment one should consider the setup illustrated in Fig. 3. Here lasers L_1 and L_2 pump

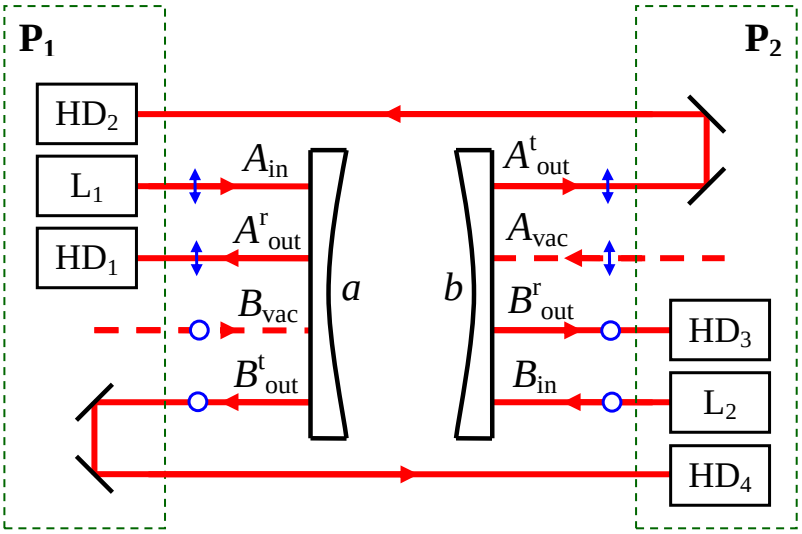

Figure 3: A double-pumped FP cavity.

the cavity with the waves $A_{\rm in}$ and $B_{\rm in}$ of orthogonal polarizations to exclude their non-linear interaction inside the cavity. $A_{\rm vac}$ and $B_{\rm vac}$ are the vacuum fields penetrating the opposite input ports. Homodyne detectors HD_1 and HD_2 measure the quadratures of the reflected and transmitted waves $A^{\rm r}_{\rm out}$ and $A^{\rm t}_{\rm out}$ correspondingly. Similarly, homodyne detectors HD_3 and HD_4 measure the quadratures of $B^{\rm r}_{\rm out}$ and $B^{\rm t}_{\rm out}$ correspondingly. Laser L_1 and both homodyne detectors HD_1 and HD_2 are assumed to be rigidly mounted on platform P_1; laser L_2 and homodyne detectors HD_3 and HD_4 are assumed to be rigidly mounted on platform P_2. Note that we make the transmitted waves return towards the emission platforms. This is done to simplify the experimental setup, since the emitting laser can also play the role of the local oscillator for detectors of both reflected and transmitted waves.

Assume for simplicity that both lasers generate optical waves with equal power and their frequencies have equal detunings from resonance (in the following we neglect the effect of the optical spring). Let us also focus on the most interesting case of the narrow-band ($\gamma\tau \ll 1$, where γ is the half-bandwidth and $\tau = L/c$) and long-wavelength approximations ($L \ll \lambda_{\rm GW}$).

After the signals (1a – 2b) are recorded they can be combined in a desirable way. In paper [5] one can find strict formulas for the reflected and transmitted signals. Formula (4) in the frequency domain taking laser and vacuum noises into account can be written as:

$$s(\omega_0+\Omega) = a_{\rm in}(\omega_0+\Omega) + b_{\rm in}(\omega_0+\Omega) + a_{\rm vac}(\omega_0+\Omega) + b_{\rm vac}(\omega_0+\Omega) - \frac{i\delta}{\gamma - i\delta}\,\mathcal{A}\,2ik_0\left[\frac{1}{2}\,Lh(\Omega) + \xi_{\rm P_2}(\Omega) - \xi_{\rm P_1}(\Omega)\right], \quad (5)$$

Here $a_{\rm in}(\omega_0+\Omega)$ and $b_{\rm in}(\omega_0+\Omega)$ are optical laser noises, $a_{\rm vac}(\omega_0+\Omega)$ and $b_{\rm vac}(\omega_0+\Omega)$ are vacuum noises, δ is the detuning of pump carrier frequency ω_0 from resonance, $\mathcal{A}$ is the amplitude of lasers, $k_0 = \omega_0/c$ is the wavenumber, $h(\Omega)$ is the GW function, $\xi_{\rm P_1}(\Omega)$ and $\xi_{\rm P_2}(\Omega)$ are the displacement noises of two platforms. Comparing Eq. (4) with Eq. (5) we come to the conclusion that p is proportional to $\delta/(\gamma - i\delta)$ which is a quantity of the order of unity if $\delta \approx \gamma$. Response (5) is written in the terms of sidebands, but in practice, of course, only quadratures can be combined. The result of such a combination will differ from (5) only in numerical factors of the order of unity.

The considered scheme suffers from at least two disadvantages:

1. Uncanceled laser noise will dominate other sources of noise in practice.
2. Displacement noise cancelation is not complete. In order to make the platform noises negligible one should somehow isolate the platforms from all sources of noise. This is hardly possible in practice. In addition, we assumed that all the optical elements (lasers, detectors, auxiliary optics) are mounted on the platforms. Otherwise, there will appear more fluctuative degrees of freedom which will even increase the residual level of displacement noise.

Laser noise can be canceled, in principle, in the balanced scheme. This usually implies detection in the dark port so that the waves interfere physically. In Fig. 4 two such balanced schemes with double-pumped cavities are demonstrated. In Fig. 4a the basic topology resembles the one of the Mach-Zehnder interferometer. Cavities are

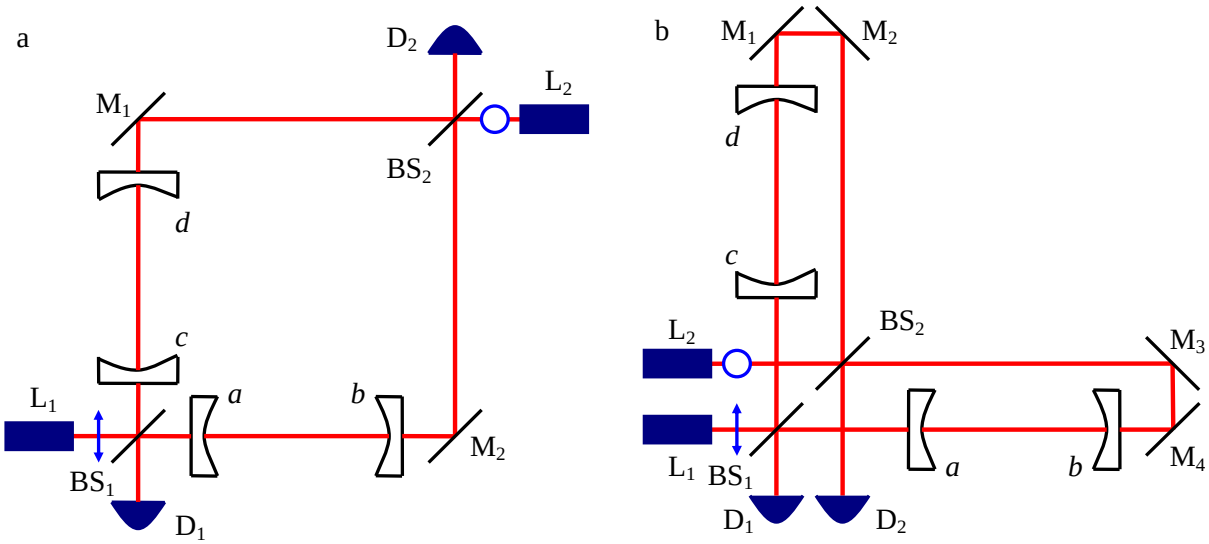

Figure 4: Balanced schemes with double-pumped cavities. a. Scheme with two "corner stations". b. Scheme with one "corner station".

inserted into two arms. Pump waves are produced by distantly located lasers (two "corner stations"). Detector D_1 registers the reflected wave corresponding to the pump of laser L_1 and the transmitted wave corresponding to the pump of laser L_2. Similarly, detector D_2 registers the reflected wave corresponding to the pump of laser

L_2 and the transmitted wave corresponding to the pump of laser L_1. In Fig. 4b the topology of the scheme is close to the conventional Michelson/Fabry-Perot topology. Both pumps are generated by closely located lasers (one "corner station") but one of the pumps is transmitted along the arms and redirected into the cavities from the other side by the additional mirrors. Detectors D_1 and D_2 perform similar to the previous case.

Although laser noise is eliminated in the proposed balanced schemes, they all suffer from the same disadvantage: their sensitivity is limited by the residual displacement noise of the beamsplitters and additional mirrors which redirect laser beams.

3.3 Resonant speed meter

3.3.1 Displacement noise cancelation at narrow frequency bands

In paper [7] it was proposed to use the concept of the speed meter as a narrow-band displacement-noise-free interferometer. Consider the scheme illustrated in Fig. 5. Laser beams of frequency ω_0 divided at the

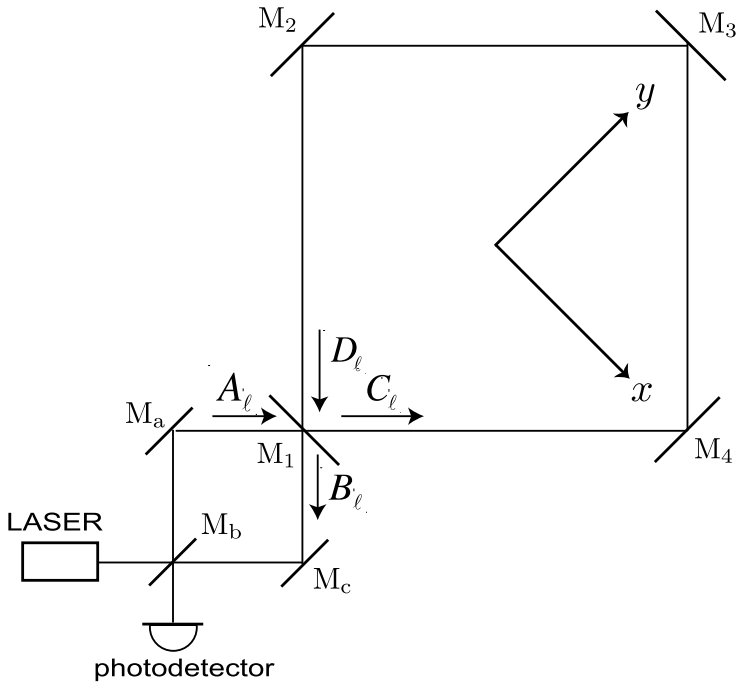

Figure 5: Resonant speed meter.

50/50 beamsplitter M_b are reflected by completely reflective mirrors M_a and M_c, and enter the (ring-shaped) synchronous recycling cavity (with arm length L), which is formed by an input mirror M_1 and three high-reflective mirrors M_2, M_3 and M_4. In the cavity, each beam circulates clockwise (CW) and counterclockwise (CCW), then leaves the cavity and is finally recombined at the beamsplitter M_b.

Consider first the recycling cavity. Mirrors M_1 and M_3 commit fluctuative motions $\eta_1(t)$ and $\eta_3(t)$ along the y-axis. Similarly, mirrors M_2 and M_4 commit fluctuative motions $\xi_2(t)$ and $\xi_4(t)$ along the x-axis. If one assumes that the resonance condition $4\omega_0\tau = 2\pi n$, $n = 1, 2, \ldots$ is fulfilled then the transfer function of the cavity for the counterclockwise can be described by the following formula:

$$\mathcal{T}^{\rm CCW}(\Omega) = -i\sqrt{2}\omega_0 \frac{R_F - R_E e^{4i\Omega\tau}}{1 - R_F R_E e^{4i\Omega\tau}} \eta_1(\Omega) + i \frac{T_F^2 R_E}{(1 - R_F R_E)(1 - R_F R_E e^{4i\Omega\tau})} \left[\delta\Psi_{\rm GW}^{\rm CCW}(\Omega) + \delta\Psi_{\rm TM}^{\rm CCW}(\Omega)\right] \quad (6)$$

Here R_F and T_F are the amplitude reflectivity and transmissivity of mirror M_1 and R_E is the composite reflectivity of mirrors M_2, M_3 and M_4; $\delta\Psi_{\rm GW}^{\rm CCW}(\Omega)$ is the GW-induced phase shift and $\delta\Psi_{\rm TM}^{\rm CCW}(\Omega)$ is the phase shift due to the displacement noise of the cavity mirrors:

$$\delta\Psi_{\rm TM}^{\rm CCW}(t) = \sqrt{2}\,\frac{\omega_0}{c}\left[-\xi_2(t-\tau) + \eta_3(t-2\tau) + \xi_4(t-3\tau) - \eta_1(t-4\tau)\right],$$

where $\tau = L/c$. A similar formula for the clockwise wave transfer function $\mathcal{T}^{\rm CW}(\Omega)$ can be written straightforwardly.

The differential signal between the CCW and CW waves is registered at the photodetector:

$$\mathcal{T}(\Omega) = \mathcal{T}^{\rm CCW}(\Omega) - \mathcal{T}^{\rm CW}(\Omega) = -i\,\frac{T_F^2 R_E}{(1-R_F R_E)(1-R_F R_E e^{4i\Omega\tau})}\left[\delta\Psi_{\rm GW}(\Omega) + \delta\Psi_{\rm TM}(\Omega)\right]. \tag{7}$$

Let us look closer at the differential phase shifts due to GW and displacement noises. The latter one takes the following form:

$$\delta\Psi_{\rm TM}(\Omega) = \delta\Psi_{\rm TM}^{\rm CCW}(\Omega) - \delta\Psi_{\rm TM}^{\rm CW}(\Omega) = 2\sqrt{2}i\,\frac{\omega_0}{c}\left[\xi_2(\Omega) + \xi_4(\Omega)\right]\sin\Omega\tau e^{2i\Omega\tau}. \tag{8}$$

Note that displacement noises $\eta_1(\Omega)$ and $\eta_3(\Omega)$ are automatically canceled out at all frequencies, because the CW and CCW beams simultaneously experience the displacements of mirrors M_1 and M_3. In addition, at the frequencies that satisfy $\Omega\tau = \pi n$, $n = 1, 2, \ldots$ all displacement noises vanish. This is because the CW and CCW beams in the cavity experience the displacement of M_2 and M_4 with the same phase, though the time of reflection is shifted by multiples of the period. Therefore, displacement noises in the cavity are not amplified around the cancelation frequencies, though the cavity is on resonance.

The GW induced phase is:

$$\delta\Psi_{\rm GW}(\Omega) = \delta\Psi_{\rm GW}^{\rm CCW}(\Omega) - \delta\Psi_{\rm GW}^{\rm CW}(\Omega) = 8i\,\frac{\omega_0}{\Omega}\,h(\Omega)\cos\Omega\tau\sin^2\frac{\Omega\tau}{2}\,e^{2i\Omega\tau}.$$

Note that the GW resonates at $\Omega = 2\pi(2m-1)/2\tau$, $m = 1, 2, \ldots$. Therefore, at $n = m = 1$ the displacement noise of the cavity is canceled (see Eq. (8)) while the GW signal is resonantly amplified.

The major limiting factor of the proposed scheme comes from the displacement noises of mirrors M_a, M_b and M_c which cannot be canceled. Their contribution to the transfer function is:

$$\mathcal{T}_{\rm add}(\Omega) = -\sqrt{2}\,\frac{\omega_0}{c}\left[\xi_a(\Omega) - \xi_b(\Omega) + \xi_c(\Omega)\right]. \tag{9}$$

Another limitation comes from the vacuum shot noise. In Fig. 6 the plots of SNR are presented.

3.3.2 Displacement noise cancelation at the wide frequency band

A narrow-band DFI speed meter can be immediately converted into a wide-band one as suggested in paper [8]. For this purpose the second pump should be introduced into the system as drawn in Fig. 7. Two lasers (with additional mirrors) are mounted on two platforms P and Q. Mirror M_3 is absolutely reflective for the beams of laser 1, while it is partially transparent for the beams of laser 2. Similarly for mirror M_1. It is evident that the beams of both laser encounter mirrors M_2 and M_4 simultaneously. Therefore, subtracting the signals of two photodetectors we obtain the signal which is completely free from displacement noise of the cavity. In the low-frequency region the DFI signal takes the following form [8, 10]:

$$s = \text{vacuum noise} + \text{platform noise} + 2\sqrt{2}\,\frac{\gamma}{\gamma - i\delta}\,\mathcal{A}\,\frac{1}{(\gamma - i\delta - i\Omega)\tau}\,ik_0\Omega\tau L h. \tag{10}$$

Here $\mathcal{A}$ is the amplitude of both lasers, γ is the half-bandwidth of the ring cavity and δ is detuning from resonance. The term "platform noise" is the displacement noise of the relative motion of the platforms P and Q along the x-axis. Residual platform noise is inevitable, because response (10) is of the 1st order (proportional to $\Omega\tau$). Both the GW signal and platform noise are comparable in magnitude and come with identical coefficients. The resonant factor $\sim \gamma\tau$ is compensated by a small factor $\sim \Omega\tau$. Again these are the consequences of the limitations imposed by the relativity principle (see Sec. 3.1).

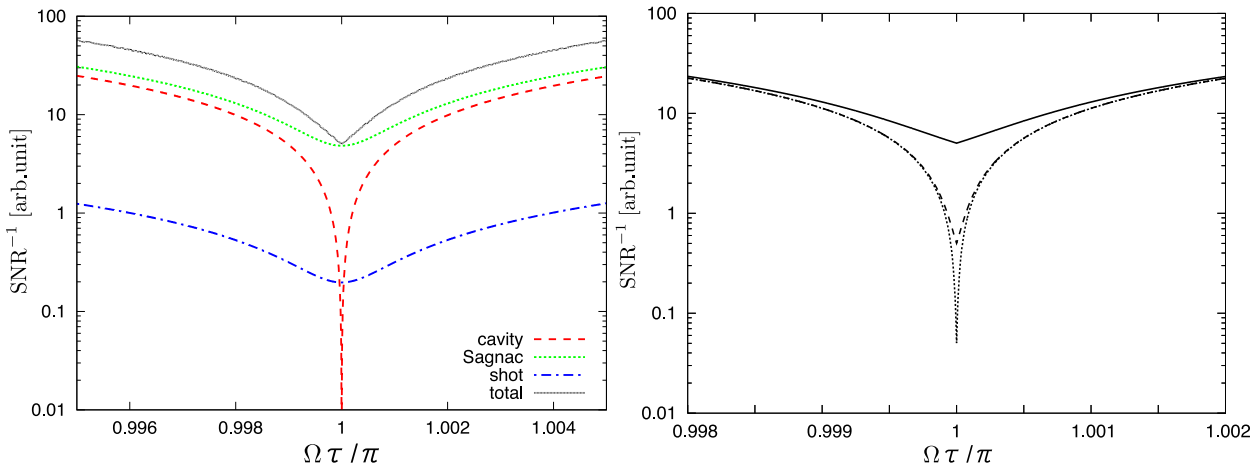

Figure 6: SNR of the resonant speed meter [7]. Left: the contribution of different noise sources to total SNR is given by the solid black curve ($R_E = 1$, $R_F = 0.99$). Right: The dependence of the SNR on the resonance factor; solid, dashed and doted curves are evaluated for $R_F = 0.99,\ 0.999,\ 0.9999$ respectively ($R_E = 1$).

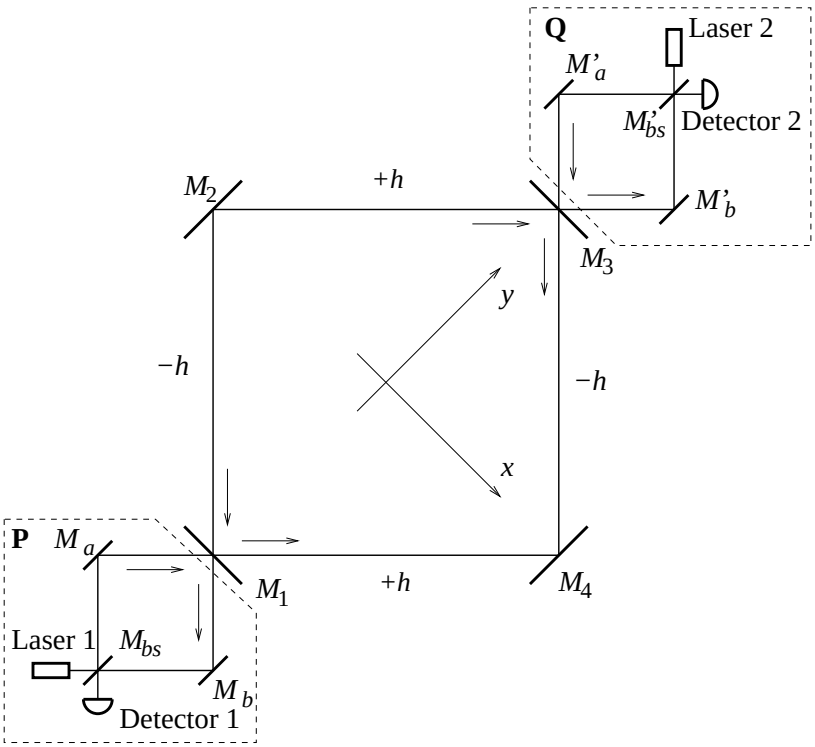

Figure 7: Wide-band displacement-noise-free resonant speed meter.

4 Complete displacement noise cancelation with cavities

4.1 Double-cavity scheme with the second order response

First let us consider a simple toy model [6] illustrated in Fig. 8. The system is composed of three test masses a,

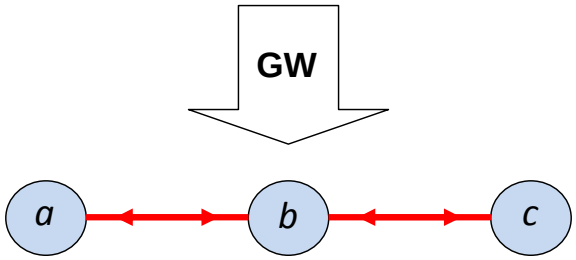

Figure 8: Three test masses in the GW field.

b and c positioned along a line. Each test mass is supplied with a laser and detector so that they can exchange electromagnetic signals and record the results. Assume all the lasers to be ideal, meaning that there is no optical laser noise. Test masses are separated by a distance L in the state of rest and commit fluctuative motions $\xi_a(t)$, $\xi_b(t)$ and $\xi_c(t)$ near the positions of equilibrium.

The phase shifts of the optical signal along the paths $a \to b \to a$ and $b \to a \to b$ are:

$$\delta\Psi_{aba}(t) = \delta\Psi_{\rm GW}(t) + k_0\big[-\xi_a(t) + 2\xi_b(t-\tau) - \xi_a(t-2\tau)\big], \tag{11}$$

$$\delta\Psi_{bab}(t) = \delta\Psi_{\rm GW}(t) + k_0\big[\xi_b(t) - 2\xi_a(t-\tau) + \xi_b(t-2\tau)\big]. \tag{12}$$

Here

$$\delta\Psi_{\rm GW}(t) = \frac{\omega_0}{2}\int_{t-2\tau}^{t} h(t_1)dt_1, \tag{13}$$

is the phase shift of the optical wave produced by the GW. From combination of phase shifts (11) and (12) one can exclude the displacement noise of test mass a in the following combination:

$$\begin{aligned} s_1(t) &= 2\delta\Psi_{aba}(t) - \delta\Psi_{bab}(t+\tau) - \delta\Psi_{bab}(t-\tau) = \\ &= 2\delta\Psi_{\rm GW}(t) - \delta\Psi_{\rm GW}(t+\tau) - \delta\Psi_{\rm GW}(t-\tau) + k_0\big[2\xi_b(t-\tau) - \xi_b(t+\tau) - \xi_b(t-3\tau)\big]. \end{aligned} \tag{14}$$

Consider now similarly platforms b and c:

$$\delta\Psi_{cbc}(t) = \delta\Psi_{\rm GW}(t) + k_0\big[\xi_c(t) - 2\xi_b(t-\tau) + \xi_c(t-2\tau)\big], \tag{15}$$

$$\delta\Psi_{bcb}(t) = \delta\Psi_{\rm GW}(t) + k_0\big[-\xi_b(t) + 2\xi_c(t-\tau) - \xi_b(t-2\tau)\big]. \tag{16}$$

The following combination of phase shifts (15) and (16) cancels displacement noise of test mass c:

$$\begin{aligned} s_2(t) &= 2\delta\Psi_{cbc}(t) - \delta\Psi_{bcb}(t+\tau) - \delta\Psi_{bcb}(t-\tau) = \\ &= 2\delta\Psi_{\rm GW}(t) - \delta\Psi_{\rm GW}(t+\tau) - \delta\Psi_{\rm GW}(t-\tau) + k_0\big[-2\xi_b(t-\tau) + \xi_b(t+\tau) + \xi_b(t-3\tau)\big]. \end{aligned} \tag{17}$$

Now we see that the GW term enters signals (14) and (17) with the same sign while the displacement noise of platform b enters with different sign. Therefore, the sum of the two signals cancels the latter:

$$s(t) = \frac{s_1(t) + s_2(t)}{2} = 2\delta\Psi_{\rm GW}(t) - \delta\Psi_{\rm GW}(t+\tau) - \delta\Psi_{\rm GW}(t-\tau). \tag{18}$$

Therefore, signal $s(t)$ represents the displacement-noise-free response of the 3-platform scheme. It should be stressed that this result does not contradict the theorem proved by Kawamura and Chen (see Sec. 2.1). In our model we assumed that timing (or, equivalently, laser) noise is absent, therefore, displacement noise cancelation in our model cannot be considered complete in the strict sense.

In the frequency domain signal (18) is:

$$s(\Omega) = -\omega_0\tau\left(1 - e^{i\Omega\tau}\right)^2 \frac{\sin\Omega\tau}{\Omega\tau}\, h(\Omega). \tag{19}$$

It is interesting to consider its long-wavelength approximation when $\Omega\tau \sim L/\lambda_{\rm GW} \ll 1$:

$$s(\Omega) \approx \omega_0\tau(\Omega\tau)^2 h(\Omega), \tag{20}$$

that corresponds to

$$s(t) \approx -\omega_0\tau\ddot{h}(t)\,\tau^2, \tag{21}$$

in time domain.

It is reasonable to expect that the FP cavities placed between the platforms will amplify the $\sim(\Omega\tau)^2$ response. However, placing cavity mirrors independently of the platforms will introduce additional 4 fluctuative degrees of freedom associated with displacement noise of the cavities. To avoid this problem it was suggested in paper [6] to mount the mirrors rigidly on the platforms. Namely, in Fig. 9 such a double-cavity scheme is demonstrated. Emission and detection in each of the cavity is performed similar to the scheme in Fig. 3 considered in Sec. 3.2.

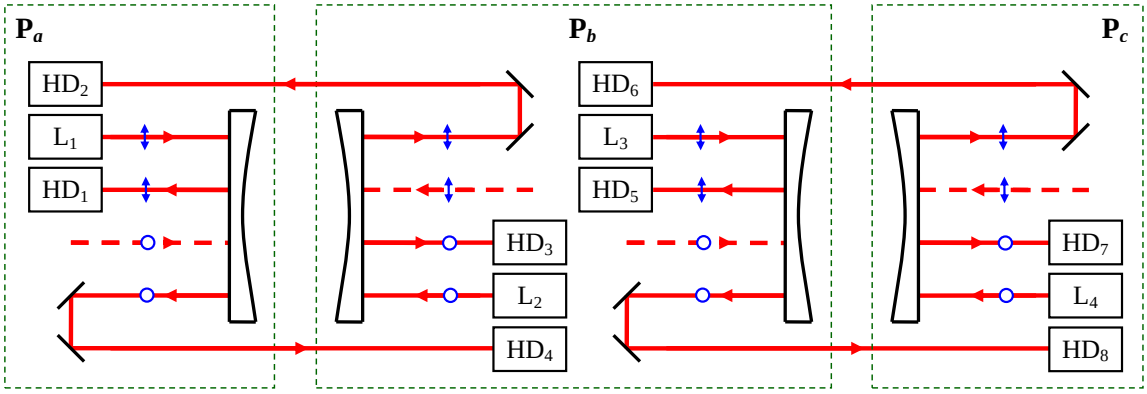

Figure 9: Double-cavity setup.

Elimination of the displacement noise of the three platforms P_a, P_b and P_c is performed in a similar way to Eqs. (14), (17) and (18). The experimentalist is free to choose whether to combine reflected signals (measured by detectors HD_1, HD_3, HD_5 and HD_7) or transmitted signals (measured by HD_2, HD_4, HD_6 and HD_8). The DFI signal takes the following form at low frequencies:

$$s = \text{laser noise} + \text{vacuum noise} + \frac{\gamma}{\gamma - i\delta}\,\mathcal{A}\,\frac{1}{(\gamma - i\delta - i\Omega)\tau}\, ik_0(\Omega\tau)^2\, Lh. \tag{22}$$

Here $\mathcal{A}$ is the amplitude of lasers, γ is the half-bandwidth of each cavity, δ is the detuning from resonance. Note that the $(\Omega\tau)^2$-multiplier is divided by a small factor of the order of $\gamma\tau$. Therefore, this is the 2nd order response with the resonant amplification. However, the susceptibility to GWs of the double-cavity DFI is still $(\Omega\tau)^2$ times worse than the one of the conventional Michelson/FP topology (such as LIGO or VIRGO).

The proposed model suffers from two major disadvantages:

1. It requires mounting of the mirrors as well as lasers and detectors on the platforms that is highly impractical, especially for the ground-based GW detectors.
2. The scheme is unbalanced, therefore laser noise cannot be canceled.

4.2 Double Michelson/Fabry-Perot interferometer with the second order response

The major disadvantages of the single-cavity scheme with the 0th order response are incomplete displacement noise cancelation and domination of laser noise. The scheme with two symmetrically positioned cavities allows complete displacement noise cancelation at the cost of a decrease of the GW susceptibility. Therefore, it is reasonable to convert this scheme into the balanced one to cancel laser noise as proposed in paper [9].

Consider the scheme illustrated in Fig. 10. Laser L pumps the interferometer with the input wave $A_{\rm L}$. Upon

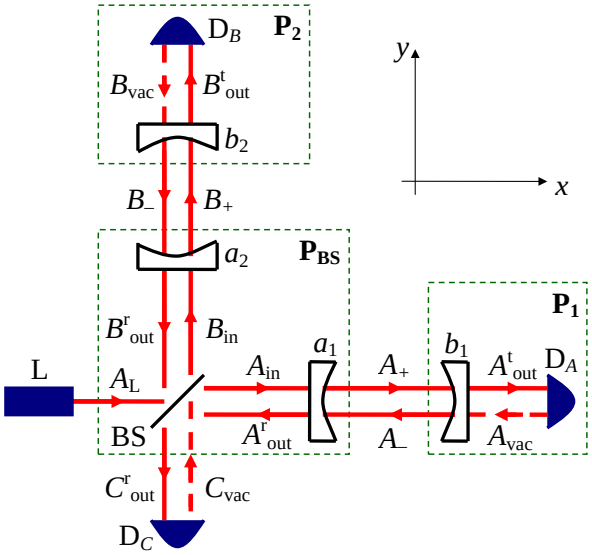

Figure 10: A Michelson/Fabry-Perot optical setup.

arrival at the 50/50-beamsplitter BS the input wave is split into two waves $A_{\rm in}$ and $B_{\rm in}$ which pump the horizontal and vertical arms, respectively. The Fabry-Perot cavity in the horizontal arm is assembled of two partially transparent mirrors a_1 and b_1. The similar cavity in the vertical arm is assembled of mirrors a_2 and b_2. Both the cavities produce reflected and transmitted waves. Reflected waves $A^{\rm r}_{\rm out}$ and $B^{\rm r}_{\rm out}$ return towards the beamsplitter and interfere. Assume the interferometer is tuned to a dark port. This means that the reflected waves interfere destructively and the mean optical power returns towards the laser. However, the weak time-dependent (signal) part $C^{\rm r}_{\rm out}$ penetrates into the dark port and falls on detector D_C. The dark port of D_C also produces the vacuum pump $C_{\rm vac}$. Transmitted waves $A^{\rm t}_{\rm out}$ and $B^{\rm t}_{\rm out}$ are measured with the corresponding detectors: in the horizontal arm it is D_A and in the vertical arm it is D_B. Both detector ports also produce the vacuum pumps $A_{\rm vac}$ and $B_{\rm vac}$.

The wave registered by D_C does not contain laser noise, only displacement noises along with the GW signal. Detector D_C may operate as the balanced homodyne detector or in the DC readout regime. In the first case local oscillation can be produced by laser L. In the second case interferometer arms should be detuned slightly so that some mean power penetrates to the dark port; since the signal is amplitude-modulated by the GW (and noises), amplitude detection is performed then by D_C and no local oscillator is required.

However, transmitted waves should be registered by the means of homodyne detection. Additional local oscillators (auxiliary lasers mounted near detectors) will be required. These lasers should be additionally synchronized with laser L in such a way that they all measure identical quadratures.

Assume that the quadratures (or amplitudes) of both transmitted waves have been measured. Once they are measured they can be stored in a computer memory and processed later. For instance, an experimentalist may produce any desired linear combinations between them. A simple subtraction of $a^{\rm t}_{\rm out}$ from $b^{\rm t}_{\rm out}$ cancels the term containing laser noise, since the latter is common for both arms. This can be thought of as a possible

method of laser noise cancelation from the transmitted waves. In the case of the reflected waves the elimination of laser noise takes place at the level of the interference of the field amplitudes and further recording of the laser-noiseless field. In the case of the transmitted waves we first record the amplitudes containing laser noise and then linearly combine them to produce the laser-noise-free quantity. However, the change in the sequence of procedures (to combine first and then record or first record and then combine) does not introduce any meaningful physical difference. However, in practice laser noise suppression by means of electronic subtraction will be mainly determined by the equality of physical parameters of photodetectors: the more identical they are, the more suppression of noise can be achieved. Computational post-processing of the recorded signals does not introduce any significant noise itself.

At this stage we have a pair of laser-noise-free signals: the one measured by the D_C and differential signal of D_A and D_B. These signals can be combined in turn to cancel one fluctuative degree of freedom. In our scheme there are four displacement noise channels: motion of the beamsplitter, differential motion of the input mirrors, differential motion of the end-mirrors and differential motion of the end-photodetectors. Therefore, we should somehow suppress two more degrees of freedom *by hands* (the last one will be eliminated by the additional interferometer, see below). We introduce the following model assumptions (see Fig. 10):

1. Both the input mirrors are rigidly attached to the beamsplitter. The composite mass will be called platform P_{BS}.
2. Detectors D_A and D_B are rigidly attached to the end-mirrors b_1 and b_2, respectively. Corresponding platforms will be called P_1 and P_2.

Let us choose to cancel the differential motion of the end-platforms P_1 and P_2. This is similar to the cancelation of the displacement noise of platform c in the 2-cavity scheme from the signals in the $b-c$ cavity. By doing so we are left only with the fluctuative motion of the cental platform P_{BS}. Let us call this partially noise-free combination $s_1(t)$. The analogy with the 2-cavity scheme suggests that the noise of the central platform can be canceled by placing the second Michelson/Fabry-Perot symmetrically.

In Fig. 11 we illustrated the scheme of double interferometer having a common cental platform. This platform

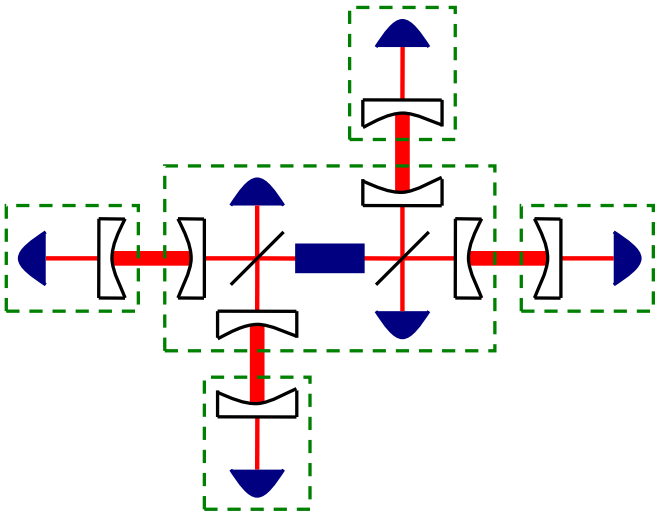

Figure 11: A double Michelson/Fabry-Perot interferometer having common central platform.

contains both beamsplitters and all the input mirrors of both interferometers mounted rigidly. The requirement of a rigid platform is crucial for our model. A single laser pumps both interferometers. Since its noise is common for both arms of each interferometer, it can be mounted independently from the central platform. In order not to complicate the figure we do not show all the additional beamsplitters and mirrors which redirect the laser

beam towards the second interferometer; these auxiliary optical elements, however, do not introduce any extra displacement noise into the signals of the second interferometer because this noise is common for both arms of the latter. Therefore, noises of these auxiliary objects are canceled either physically by the interference in the dark port, or electronically when subtracting one transmitted signal from another. Due to this reason all the objects which are encountered by the optical wave before it falls on the main beamsplitter of the Michelson interferometer do not introduce their displacement noise into the laser-noise-free signals, and thus can be, in principle, detached from the platform (similar to the laser itself).

We assume that the procedure of noise-cancelation of the end-platforms has also been performed for the second interferometer resulting in partially noise-free signal $s_2(t)$. Finally adding the responses $s_1(t)$ and $s_2(t)$ we obtain the displacement-noise-free signal $s(t)$ which takes the following form in the low-frequency region (long-wavelength approximation):

$$s = \text{vacuum noise} - \frac{\gamma}{\gamma - i\delta}\,\mathcal{A}\,ik_0\Omega\tau\,\frac{1}{2}\,Lh. \tag{23}$$

Here $\mathcal{A}$ is the amplitude of the laser, γ is the cavity half-bandwidth, δ is the detuning from resonance. One may conclude from formula (23) that the GW susceptibility of the proposed scheme is $(\Omega\tau)$ times worse than the one of Michelson interferometer. Although all displacement noises have been canceled, the first order response indicates that uncanceled laser noise remains — the noise of local oscillators which are used for detection of the transmitted signals. An attempt to make transmitted waves interfere and detect the dark-port signal leads to the rise of displacement noise of the mirrors that redirect the waves.

Note also that the GW signal in formula (23) comes without the resonant gain. Therefore, the loss of the sensitivity of the proposed DFI topology in comparison to the conventional Michelson/FP topology at $f_{\rm GW} \sim 100$ Hz can be estimated as $\sim 10^{-4}$ by the order of magnitude if the cavity half-bandwidth $\gamma/2\pi \sim 100$ Hz and $L = 10$ km. Due to this reason one may conclude that the proposed topology has no advantages over Michelson/FP topology for the purpose of the ground-based GW detection.

5 Conclusion

We have reviewed most of the displacement noise reduction techniques present in literature. Clearly, at the moment none of the proposed schemes is valid for immediate implementation in practice. The general peculiarity of displacement-noise free interferometers is the decrease of the GW susceptibility in the low frequency region ($L/\lambda_{\rm GW} \ll 1$). This drawback comes from the mechanism of noise cancelation. Fortunately, when all displacement and laser noises are canceled (or strongly suppressed) the only limiting factor becomes vacuum shot noise which can be depressed by increase of laser amplitude of squeezing. In addition, several DFI schemes that implement the cavities allow resonant amplification of the GW response. However, the schemes with resonantly amplified GW response suffer from other disadvantages such as uncanceled laser noise (which is dominant in practice) or requirement of rigid platforms (that are very impractical). Although these limitations could be overcome, in principle, the significant loss of the GW susceptibility in low-frequency region does not allow the displacement noise reduction schemes, considered in this review, to have advantages over conventional (non-DFI) topologies for the means of the ground-based GW detection.

A Mechanism of displacement noise cancelation

A.1 Inertial reference test mass

Let us choose one of the interferometer's photodetectors (D) as the reference test mass (TM). First we consider the case of the inertial photodetector, i.e. the one which strictly follows the geodesic of the GW. It the photodetector's local Lorentz frame interaction of an interferometer with the GW adds up to two effects (see [11, 12, 13]). Correspondingly, the response of an interferometer (phase shift) can be represented as a sum of two terms. The first effect, which corresponds to a phase shift $\delta\Psi_{\mathrm{GW+TM}}(t)$, is the motion of the test masses in the tidal force-field of the GW. If the j-th test mass is located at a distance $L_j = c\tau_j$ away from the photodetector then its GW-induced displacement $\frac{1}{2}L_j h(t)$ enters in $\delta\Psi_{\mathrm{GW+TM}}(t)$ as $a_j k_0 \frac{1}{2} L_j h(t - n_j\tau_j)$. This is because the information about the motions of the test masses, separated by a distance L_j, cannot be transferred between them faster than L_j/c in any force-field. Coefficients a_j take into account the peculiarities of the interferometer's geometry, and natural numbers n_j take into account the time delays corresponding to this geometry. If an interferometer consists of N test masses then:

$$\delta\Psi_{\mathrm{GW+TM}}(t) = \sum_{j=1}^{N} a_j k_0 \frac{1}{2} L_j h(t - n_j\tau_j). \tag{24}$$

Note that the summand corresponding to the photodetector itself does not enter this formula, since by definition we work in its local Lorentz frame where $L_{\mathrm{D}} = 0$.

All the forces acting on the test masses, including the GW force, are indistinguishable by interferometry, since they change the phases of the optical waves only at the moments of reflection. From the point of view of interferometry this property of the forces describe their localized (in space and time) nature. Let us denote the fluctuative displacement of the j-th test mass under the influence of all non-GW forces as $\xi_j(t)$. The corresponding phase shift will be denoted as $\delta\Psi_{\mathrm{TM\ fluct}}(t)$. Due to the indistinguishability between the GW and non-GW forces the latter can be written in the following form:

$$\delta\Psi_{\mathrm{TM\ fluct}}(t) = \sum_{j=1}^{N} a_j k_0 \xi_j(t - n_j\tau_j). \tag{25}$$

Here the summand corresponding to the fluctuative motion of the photodetector cancels out, since it is an inertial test mass by definition and therefore, $\xi_{\mathrm{D}}(t) = 0$. Total contribution of the localized effects (displacement of the test masses) into the interferometer's response can be written in the following form:

$$\delta\Psi_{\mathrm{TM}}(t) = \delta\Psi_{\mathrm{GW+TM}}(t) + \delta\Psi_{\mathrm{TM\ fluct}}(t) = \sum_{j=1}^{N} a_j k_0 \left[\frac{1}{2} L_j h(t - n_j\tau_j) + \xi_j(t - n_j\tau_j)\right], \tag{26}$$

or in the frequncy domain:

$$\delta\Psi_{\mathrm{TM}}(\Omega) = \delta\Psi_{\mathrm{GW+TM}}(\Omega) + \delta\Psi_{\mathrm{TM\ fluct}}(\Omega) = \sum_{j=1}^{N} a_j k_0 \left[\frac{1}{2} L_j h(\Omega) + \xi_j(\Omega)\right] e^{in_j\Omega\tau_j}. \tag{27}$$

If the linear scale of the GW detector $L = c\tau$[2] is far less than the gravitational wavelengths λ_{GW} (long-wavelength approximation), i.e. $L_j \sim L \ll \lambda_{\mathrm{GW}}$ for all j, then it is convenient to expand the exponents corresponding to

[2]Usually arms lengths L_j of the GW antennas are chosen to be the multiples of fixed length L, i.e. $L_j = \alpha_j L$, where α_j — numbers. Therefore, L can be considered as a typical length-scale, and typical trip time $\tau = L/c$.

time delays into Taylor series in the vicinity of zero:

$$\delta\Psi_{\rm TM}(\Omega) = \sum_{j=1}^{N} a_j k_0 \left[\frac{1}{2} L_j h(\Omega) + \xi_j(\Omega)\right] \left[1 + in_j\Omega\tau_j + \frac{(in_j\Omega\tau_j)^2}{2} + \ldots\right] =$$
$$= \sum_{j=1}^{N} a_j k_0 \left[\frac{1}{2} L_j h(\Omega) + \xi_j(\Omega)\right] \left[b_{0j}(\Omega\tau_j)^0 + b_{1j}(\Omega\tau_j)^1 + b_{2j}(\Omega\tau_j)^2 + \ldots\right]. \quad (28)$$

Here the numerical multipliers b_{ij} take into account the coefficients of the Taylor expansion with $b_{0j} \equiv 1$. It is clear that in the long-wavelength approximation the GW response has the order of $h(\Omega\tau)^0 \sim h(L/\lambda_{\rm GW})^0$ (these are the terms of the 0th order in the Taylor expansion), where h is the typical value of the GW amplitude. In addition, due to the time delays L/c there appear the terms of the order of $O[h(L/\lambda_{\rm GW})^1]$ in the response.

It is convenient to represent the time delays τ_j in the form $\alpha_j\tau$, where α_j are the numerical coefficients. Then $\delta\Psi_{\rm TM}(\Omega)$ can be rewritten as:

$$\delta\Psi_{\rm TM}(\Omega) = \sum_{k=0}^{\infty} \mathcal{G}_k(\Omega)(\Omega\tau)^k + \sum_{k=0}^{\infty} \mathcal{N}_k(\Omega)(\Omega\tau)^k, \quad (29)$$

where

$$\mathcal{G}_k(\Omega) = \sum_{j=1}^{N} a_j k_0 \frac{1}{2} L_j h(\Omega) b_{kj} (\alpha_j)^k, \qquad \mathcal{N}_k(\Omega) = \sum_{j=1}^{N} a_j \xi_j(\Omega) b_{kj} (\alpha_j)^k. \quad (30)$$

Functions $\mathcal{G}_k(\Omega)$ and $\mathcal{N}_k(\Omega)$ describe the action of the GW force and all the non-GW forces correspondingly. From Eq. (29) it explicitly follows that the GW and non-GW forces are indistinguishable in all orders of $\Omega\tau \sim L/\lambda_{\rm GW}$.

The second effect of the GW in the local Lorentz frame is their direct interaction with the optical waves. This can be qualitatively interpreted as the propagation of the optical waves in the medium with effective refraction index [11, 12]. While traveling in such a (boundless) medium the optical wave acquires the corresponding phase shift $\delta\Psi_{\rm GW+EMW}(t)$ gradually, meaning that this is a distributed (in space and time) effect. In the long-wave approximation the direct interaction of the GWs with light is an effect of the $O[h(L/\lambda_{\rm gw})^2]$ order [12]. In other words, introducing some numerical coefficients c_k, the corresponding phase shift can be written in the following form:

$$\delta\Psi_{\rm GW+EMW}(\Omega) = \sum_{k=2}^{\infty} k_0 L h(\Omega) c_k (\Omega\tau)^k \equiv \sum_{k=2}^{\infty} \tilde{\mathcal{G}}_k(\Omega)(\Omega\tau)^k. \quad (31)$$

The response $\delta\Psi(\Omega)$ of an interferometer, as discussed above, is the sum of the response to displacements of the test masses $\delta\Psi_{\rm TM}(\Omega)$ and the response to distributed effect of GW $\delta\Psi_{\rm GW+EMW}(\Omega)$:

$$\delta\Psi(\Omega) = \delta\Psi_{\rm TM}(\Omega) + \delta\Psi_{\rm GW+EMW}(\Omega) =$$
$$= \sum_{k=0}^{\infty} \mathcal{G}_k(\Omega)(\Omega\tau)^k + \sum_{k=0}^{\infty} \mathcal{N}_k(\Omega)(\Omega\tau)^k + \sum_{k=2}^{\infty} \tilde{\mathcal{G}}_k(\Omega)(\Omega\tau)^k =$$
$$= (\mathcal{G}_0 + \mathcal{N}_0)(\Omega\tau)^0 + (\mathcal{G}_1 + \mathcal{N}_1)(\Omega\tau)^1 + (\mathcal{G}_2 + \tilde{\mathcal{G}}_2 + \mathcal{N}_2)(\Omega\tau)^2 + (\mathcal{G}_3 + \tilde{\mathcal{G}}_3 + \mathcal{N}_3)(\Omega\tau)^3 + \ldots \quad (32)$$

it follows that beginning from the 2nd order of $L/\lambda_{\rm GW}$ it is possible, in principle, to distinguish the influence of the GW on an interferometer from the fluctuative forces. Note, however, that the first non-vanishing term in the noise-free linear combination of the interferometer's responses can be of the higher (than the second) order of smallness due to specific topology of the GW DFI detector.

Therefore, from the viewpoint of the local Lorentz frame displacement-noise-free interferometry implies cancelation of the localized effects (GW and non-GW forces), leaving only the distributed effect (direct interaction of the GW with light).

A.2 Non-inertial reference test mass

Now let us consider the case of the photodetector to be subjected to the external fluctuative forces. This means that the proper reference frame is non-inertial and we have to take this fact into account.

In the photodetector's proper reference frame the fluctuative motion of the j-th test mass equals to $\delta x_j(t) = \xi_j(t) - \xi_{\rm D}(t)$ [13]. The corresponding phase shift $\delta\Psi_{\rm TM\ fluct}(t)$ takes the form:

$$\delta\Psi_{\rm TM\ fluct}(t) = \sum_{j=1}^{N} a_j k_0 \delta x_j(t - n_j\tau_j). \tag{33}$$

The phase shift $\delta\Psi_{\rm GW+TM}(t)$ remains unchanged. Therefore, the phase shift due to the displacements of the test masses takes the following form:

$$\delta\Psi_{\rm TM}(\Omega) = \sum_{k=0}^{\infty} \mathcal{G}_k(\Omega)(\Omega\tau)^k + \sum_{k=0}^{\infty} \mathcal{N}_k(\Omega)(\Omega\tau)^k, \tag{34}$$

$$\mathcal{G}_k(\Omega) = \sum_{j=1}^{N} a_j k_0 \frac{1}{2} L_j h(\Omega) b_{kj}(\alpha_j)^k, \qquad \mathcal{N}_k(\Omega) = \sum_{j=1}^{N} a_j \delta x_j(\Omega) b_{kj}(\alpha_j)^k, \tag{35}$$

with all the numerical coefficients remaining unchanged.

The major difference from the previous case of an inertial reference is that the optical wave directly interacts with the effective gravitational field of the non-inertial frame. According to Ref. [13] this interaction has a distributed nature. The corresponding phase shift has the order of $O[k_0(\Omega\tau)^2\xi_{\rm D}]$, therefore it can be written in the following form:

$$\delta\Psi_{\rm acc+EMW}(\Omega) = \sum_{k=2}^{\infty} k_0 \xi_{\rm D}(\Omega) d_k (\Omega\tau)^k \equiv \sum_{k=2}^{\infty} \tilde{\mathcal{N}}_k(\Omega)(\Omega\tau)^k, \tag{36}$$

where d_k are some numerical coefficients. The total response of an interferometer takes the form::

$$\begin{aligned}\delta\Psi(\Omega) = \sum_{k=0}^{\infty} \mathcal{G}_k(\Omega)(\Omega\tau)^k + \sum_{k=0}^{\infty} \mathcal{N}_k(\Omega)(\Omega\tau)^k + \sum_{k=2}^{\infty} \tilde{\mathcal{G}}_k(\Omega)(\Omega\tau)^k + \sum_{k=2}^{\infty} \tilde{\mathcal{N}}_k(\Omega)(\Omega\tau)^k = \\ = (\mathcal{G}_0 + \mathcal{N}_0)(\Omega\tau)^0 + (\mathcal{G}_1 + \mathcal{N}_1)(\Omega\tau)^1 + (\mathcal{G}_2 + \tilde{\mathcal{G}}_2 + \mathcal{N}_2 + \tilde{\mathcal{N}}_2)(\Omega\tau)^2 + \dots\end{aligned} \tag{37}$$

It follows that the new fluctuative term appears beginning from the 2nd order of $\Omega\tau$ having a distributed nature. However, the structure of formulas for $\delta\Psi_{\rm GW+EMW}(\Omega)$ and $\delta\Psi_{\rm acc+EMW}(\Omega)$ (see [13]) tells thatthe corresponding functions $\tilde{G}_k(\Omega)$ and $\tilde{N}_k(\Omega)$ cannot coincide for all k. Therefore, beginning from some $k \geq 2$ it is possible, in principle, to distinguish the GW from the fluctuative motions of the test masses.

Summing up, in the case of a non-inertial reference test mass one cannot consider the action of external force on an interferometer as a localized effect. However, in Ref. [13] it was shown that in all ultimate results the sum $\delta\Psi_{\rm TM\ fluct}(\Omega) + \delta\Psi_{\rm acc+EMW}(\Omega)$ either coincides with

$$\delta\Psi_{\rm TM\ fluct}(\Omega) + \delta\Psi_{\rm acc+EMW}(\Omega) = \sum_{k=0}^{\infty} \mathcal{N}_k(\Omega)(\Omega\tau)^k + \sum_{k=2}^{\infty} \tilde{\mathcal{N}}_k(\Omega)(\Omega\tau)^k = \sum_{j=1}^{N} a_j k_0 \xi_j e^{in_j\Omega\tau_j}, \tag{38}$$

for the round-trip schemes, or differs in the Doppler correction (due to the motion of the reference test mass) for the forward-trip schemes. Therefore, the displacement noise of the reference test mass enters the response of an interferometer as the localized effect, although it is calculated is a distributed one. Due to this reason we consider the GW as the only distributed effect.

...

References

[1] S. Kawamura and Y. Chen, "Displacement-Noise-Free Gravitational-Wave Detection", Phys. Rev. Lett. **93**, 211103, 2004. 2, 3

[2] Y. Chen and S. Kawamura, "Displacement- and Timing-Noise Free Gravitational-Wave Detection", Phys. Rev. Lett. **96**, 231102, 2006. 2, 4

[3] Y. Chen *et al.*, "Interferometers for Displacement-Noise-Free Gravitational-Wave Detection", Phys. Rev. Lett. **97**, 151103, 2006. 2, 3, 4, 5

[4] K. Somiya *et al.*, "Utility investigation of artificial time delay in displacement-noise-free interferometers", Phys. Rev. D **76**, 022002, 2007. 2, 5

[5] S.P. Tarabrin and S.P. Vyatchanin, "Displacement-noise-free gravitational-wave detection with a single Fabry-Perot cavity: a toy model", Phys. Lett. A **372**, 6801, 2008. 2, 10

[6] A.A. Rakhubovsky and S.P. Vyatchanin, "Displacement-noise-free gravitational-wave detection with two Fabry-Perot cavities", Phys. Lett. A **373**, 13, 2008. 3, 14, 15

[7] A. Nishizawa, S. Kawamura and M. Sakagami, "Resonant Speed Meter for Gravitational-Wave Detection", Phys. Rev. Lett. **101**, 081101, 2008. 3, 11, 13

[8] S.P. Vyatchanin, "Displacement-noise-free resonant speed meter for gravitational-wave detection", arXiv:0808.3445v1. 3, 12

[9] S.P. Tarabrin and S.P. Vyatchanin, "Double Michelson/Fabry-Perot interferometer for laser- and displacement-noise-free gravitational-wave detection", arXiv:0904.3296v1. 3, 16

[10] S.P. Vyatchanin, private communication. 12

[11] M. Rakhmanov, "'Response of test masses to gravitational waves in the local Lorentz gauge", Phys. Rev. D **71**, 084003, 2005. 20, 21

[12] S.P. Tarabrin, "Interaction of plane gravitational waves with a Fabry-Perot cavity in the local Lorentz frame", Phys. Rev. D **75**, 102002, 2007. 20, 21

[13] S.P. Tarabrin and A.A. Seleznyov, "Optical position meters analyzed in the noninertial reference frames", Phys. Rev. D **78**, 062001, 2008. 20, 22